Chemical Papers (2020) 74:3589–3595
https://doi.org/10.1007/s11696-020-01192-4

ORIGINAL PAPER

Determination of stoichiometry and stability constants of iron complexes of phenanthroline, Tris(2-pyridyl)-s-triazine, and salicylate using a digital camera

Ahmed A. Shalaby[1] · **Ashraf A. Mohamed**[1]

Received: 28 January 2020 / Accepted: 7 May 2020 / Published online: 16 May 2020

Abstract
The determination of stoichiometric ratios and stability constants of metal–ligand complexes is of great importance for physical, chemical, biochemical, and environmental studies and often require relatively expensive and sophisticated instruments. Herein, we introduce a simple, accurate, and low-cost method for determining these parameters by a conventional digital camera. The stoichiometric ratios and stability constants of iron complexes of 1,10-phenanthroline, 2,4,6-Tris(2-pyridyl)-s-triazine, and salicylate were determined, as model examples, using the molar ratio and the continuous variation methods. Digital images of solutions with various metal–ligand ratios were captured and analyzed, and the Y_{xy} color absorbance and the ΔE_{LUV} color difference parameters were used as convenient analytical signals that favorably compete with conventional spectrophotometric signals. For the three studied iron complexes, the results of stoichiometric ratios and stability constants obtained from digital images were in excellent agreement with the spectrophotometric and the previously reported literature's data.

Keywords Digital imaging · Y_{xy}color absorbance · ΔE_{LUV} color difference · Stability constant · Metal complexes · Absorption spectra

Introduction

The stoichiometry and stability constants of metal complexes are important parameters for physical, chemical, biochemical, and environmental studies. Different techniques were used for the determination of these parameters including UV–VIS spectrophotometry (Carmody 1964; Chattopadhyaya and Singh 1974; Dömötör et al. 2018; Gamov et al. 2019; Kluska et al. 2018; Kocyla et al. 2017; Ravichandran et al. 2014), spectrofluorimetry (Chen et al. 2015; Cuprys et al. 2018), potentiometry (Dömötör et al. 2018; Friend and Wall 2019; Jakusch 2018; JANRAO et al. 2014; Kluska et al. 2018; Kocyla et al. 2017; S. Al–Farhan 2018), voltammetry (Geiger et al. 1991; Kamyabi et al. 2016), conductometry (Kazemi et al. 2016; Al–Farhan 2018), gel chromatography (Yoza 1977), ion exchange chromatography (Wacker and Seubert 2014), liquid–liquid extraction (Omoto and Wall 2017), electrophoresis (Ansorge et al. 2018; Holm et al. 2013; TEWARI' et al. 1993), and isothermal calorimetry (Holm et al. 2013; Kluska et al. 2018). These techniques often require sophisticated and relatively expensive instruments, where the very popular UV–VIS spectrophotometry is most commonly used. Stoichiometry and stability constants can be determined spectrophotometrically by several methods including the Job's continuous variation method (Carmody 1964), the molar ratio method, and the Bjerrum method. (JANRAO et al. 2014).

Recently, digital imaging devices, e.g., digital cameras (Mohamed and Shalaby 2019; Mohamed et al. 2018), smartphone cameras (Dutta 2019; Mohamed and Shalaby 2019; Mohamed et al. 2018), and scanners (Mohamed and Shalaby 2019; Mohamed et al. 2018; Shokrollahi et al. 2015), served as sensors for colorimetric analysis. Captured images were analyzed to yield the Red, Green, and Blue (RGB) channel intensities (de Morais et al. 2016; Huangfu

Electronic supplementary material The online version of this article (https://doi.org/10.1007/s11696-020-01192-4) contains supplementary material, which is available to authorized users.

✉ Ashraf A. Mohamed
aamohamd@sci.asu.edu.eg

[1] Department of Chemistry, Faculty of Science, Ain Shams University, Abbassia, Cairo 11566, Egypt

et al. 2019; Mohamed and Shalaby 2019; Mohamed et al. 2018). Recently, Morais et al. (de Morais et al. 2016) applied the red color channel intensity as a signaling tool for the determination of the Iron-Phenanthroline binding constant. However, the channel intensities of the non-uniform RGB color space were characterized by poor calibration linearity (Mohamed and Shalaby 2019; Mohamed et al. 2018) and therefore were mathematically converted into the $Y_{xy}$and ΔE_{LUV} color space signals that gave excellently linear calibration responses that favorably competed with signals of sophisticated spectrophotometers (Mohamed and Shalaby 2019; Mohamed et al. 2018).

Here we describe a low-cost, simple, sensitive, and accurate method for the determination of the stoichiometry and stability constants of metal–ligand complexes using digital image-based analysis (DIBA). The stoichiometric ratios and stability constants of the Iron complexes with 1,10-Phenanthroline (Phen), 2,4,6-Tris(2-pyridyl)-s-triazine (TPTZ), and Salicylate (SAL) were determined using the molar ratio and the continuous variation methods. A conventional digital camera was used to capture images of cuvettes containing reacting solutions of the iron complexes with various Fe/L ratios or mole fraction. Captured images were analyzed to obtain the non-uniform RGB color space parameters that were converted to the corresponding $Y_{xy}$and $\Delta \mathrm{E_{LUV}}$ color space analytical signals.(Mohamed and Shalaby 2019; Mohamed et al. 2018) The Y_{xy} color absorbance and $\Delta \mathrm{E_{LUV}}$ color difference values were plotted against the molar ratio or the mole fraction and the stoichiometric ratio and stability constant values were calculated.

Theoretical

The formation of mononuclear complexes can be represented by the following chemical equilibrium $\mathrm{M} + \mathrm{nL} \leftrightarrow \mathrm{MLn}$.

The stability constant β_n is given by Eq. (1). In most cases one of the reaction constituents takes part in other equilibrium reaction, e.g., the ligand can be protonated or competed by other metal ions present, so the real concentration of the free ligand may differ widely in solutions with the same total ligand concentration. In this case, the apparent stability constant is called a conditional stability constant "β_n'" and the overall stability constant can be calculated using Eq. (2) (Chattopadhyaya and Singh 1974; Inczédy 1976). Where $\alpha_{L(H)}$ is the side reaction function of ligand protonation and can be calculated using Eq. (3) (Chattopadhyaya and Singh 1974).

$$\beta_n = \frac{[ML_n]}{[M][L]^n} \tag{1}$$

$$\beta_n = \beta_n'(\alpha_{L(H)})^n \tag{2}$$

$$\alpha_{L(H)} = 1 + \frac{[H^+]}{K_1} + \frac{[H^+]^2}{K_1 K_2} + \ldots \tag{3}$$

The conditional and overall stability constants can be determined from the plots of the molar ratio and continuous variation methods, where at the point of stoichiometry, the ratio between the true observed absorbance (or color absorbance, or color difference) (A_t) to that extrapolated by the tangents (A_{ex}) equal to the mole fraction of the metal ion or the ligand in the complex, Eq. (4). Thus, the concentration of the complex species can be expressed by Eq. (5), and the concentration of the free metal ion and the free ligand can be expressed by Eqs. (6) and (7), respectively. Thus, by substitution in Eq. (1), the conditional stability constant can be calculated from Eq. (8).(Inczédy 1976)

$$\frac{A_t}{A_{ex}} = \frac{[ML_n]}{C_M} = \frac{n[ML_n]}{C_L} \tag{4}$$

$$[ML_n] = \frac{A_t}{A_{ex}} C_M \tag{5}$$

$$[M] = C_M - \frac{A_t}{A_{ex}} C_M \tag{6}$$

$$[L] = C_L - n\frac{A_t}{A_{ex}} C_M \tag{7}$$

$$\beta_n' = \frac{[ML_n]}{[M][L]^n} = \frac{\frac{A_t}{A_{ex}} C_M}{\left[C_M - \frac{A_t}{A_{ex}} C_M\right]\left[C_L - n\frac{A_t}{A_{ex}} C_M\right]^n} \tag{8}$$

where C_M and C_L are the analytical concentrations of the metal and ligand, whereas $[M]$, $[L]$, and $[ML_n]$ are the equilibrium concentrations of the metal, ligand, and complex, respectively.

Experimental

Apparatus and software

Digital Image-Based Analysis (DIBA) measurements were made using a simple homemade platform. (Mohamed and Shalaby 2019; Mohamed et al. 2018) In brief, the platform consisted of (1) two matched 10 mm glass cells (2) the digital camera and (3) a white cartoon paper as background diffuser. The diffuser, the 3D printed cell-holder and the camera

were fixed on a 20 × 20 cm wood plate; each of them was 5-cm distance apart. Digital images were captured, on the bench of our laboratory, using a Canon PowerShot A810 digital camera that is equipped with a 16.0 Mega Pixel CCD sensor, where the conventional fluorescent daylight-lamp fixed to the ceiling served as the light source. (Mohamed and Shalaby 2019; Mohamed et al. 2018) A conventional HP-EliteBook 2540P notebook running under windows 10 was used for treatment of data and analysis. Photoshop CC 2017 and imageJ 1.52c software were used for digital image cropping and RGB channel intensities calculations, respectively. The obtained RGB intensities were converted into the corresponding coordinates of the Y_{xy} and LUV color spaces using the free colormine online converter (Colormine color converter. 2019).

Spectrophotometric measurements, for comparison only, were made on a Shimadzu 1650 UV/VIS spectrophotometer controlled by an UVProbe-2.5 software (Kyoto, Japan).

Eppendorf 10-100 and 100-1000 µL vary-pipettes (Westbury, NY, USA) and a calibrated EDT pH-mV meter (Dover Kent, UK) were used.

Materials and chemicals

All reagents were of ACS grade and were used as received from Sigma-Aldrich (St. Louis, MO, USA), Merck (Darmstadt, Germany) or BDH (Poole, UK). Unless otherwise stated, de-ionized water and aqueous solutions were used throughout. *1,10*-phenanthroline, *2,4,6*-Tris(2-pyridyl)-s-triazine, sodium salicylate, ferrous ammonium sulfate hexahydrate, ferric ammonium sulfate dodecahydrate, and L-ascorbic acid, sodium acetate, sodium nitrate, and concentrated H_2SO_4, concentrated HNO_3 were also used.

Determination of stoichiometry and stability constants of the iron complexes

For the determination of Fe(II)-Phen stoichiometry using the molar ratio method, the following solutions were used: (1) 100 mL solutions of Fe(II) 6.00×10^{-4} mol L^{-1}, and (2) 100 mL Phen solution 6.00×10^{-4} mol L^{-1}. In a series of dry 10 mm path length glass spectrophotometric cells, 200 µL aliquots of Fe(II) were mixed with 300 µL of 1.0% *w/v* ascorbic acid [to reduce any Fe(III) traces present in the Fe(II)] and 300 µL of 1.0 mol L^{-1} acetate buffer (pH = 3.5). Increasing volumes of Phen (0 to 1200 µL) were then added to the reaction cuvettes to give increasing [Phen]/[Fe] ratios from 0.0 to 6.0. The reacting solutions were diluted with water to exactly 3000 µL and then mixed well. All measurements were made at 25 °C with the ionic strength adjusted to 0.1 mol L^{-1} using sodium nitrate solution.

For the determination of Fe(II)-Phen stoichiometry using the Job's method, 3.00×10^{-4} mol L^{-1} solutions of Fe(II) and Phen were used. In another series of dry 10 mm path length glass spectrophotometric cells, various volumes of Fe(II) (100 to 1900 µL) and Phen (1900 to 100 µL) were mixed to give the desired mole fractions. A 300 µL of each of ascorbic acid and acetate buffer (pH = 3.5) was added, and the final volume of each cuvette was then diluted to 3000 µL with water and the reacting solutions were mixed well. Similarly, all measurements were made at 25 °C with the ionic strength adjusted to 0.1 mol L^{-1} using sodium nitrate solution.

The molar ratio and the continuous variation methods were similarly followed for the Fe(II)-TPTZ and Fe(III)-SAL systems. However, the appropriate experimental conditions of the respective procedures were used. Namely, for the Fe(II)-TPTZ system, 3.80×10^{-4} and 1.00×10^{-4} mol L^{-1} Fe(II) solutions were used for the molar ratio and the continuous variation methods, respectively. Moreover, acetate buffer of pH 4.5 was used. However, for the Fe(III)-SAL system, 1.80×10^{-3} mol L^{-1} Fe(III) solution was used for both the molar ratio and the continuous variation methods. Further, 50 µL of 0.10 mol L^{-1} nitric acid was used to adjust the medium acidity, in the latter system.

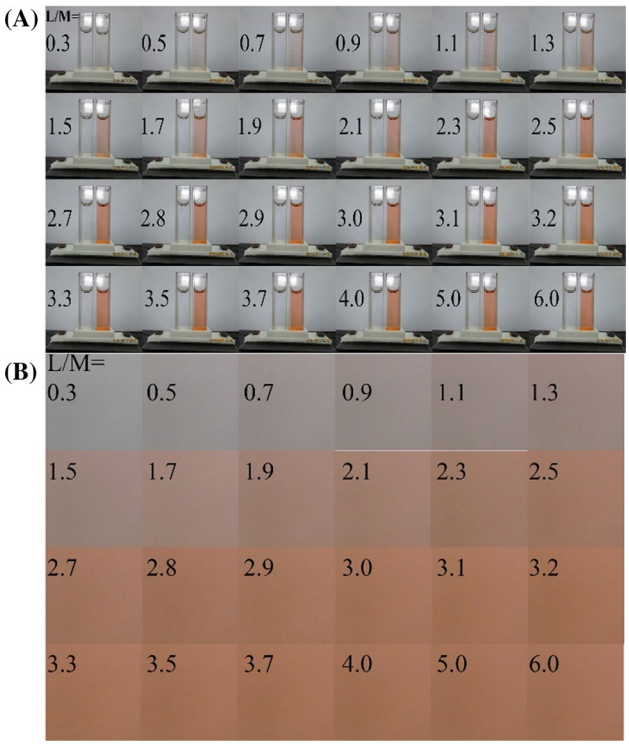

Fig. 1 Digital images of Fe(II)-phenanthroline complex at different [phenanthroline]/[Fe(II)] molar ratio (**a**) and the cropped Area of interest (**b**). Except for the studied variable, other conditions were those given in th recommended procedure. Captured images were arbitrarily compressed to fit into the page margins; however, for image analysis, the original uncompressed images were used

Results and discussion

Spectra and Image acquisition

In the molar ratio method, solutions having various [*L*]/[*M*] molar ratios were prepared for the Fe(II)-Phen, Fe(II)-TPTZ, and Fe(III)-SAL complexes. A portion from each solution was placed in the spectrophotometric cell and was placed in our homemade platform to capture respective digital images that were automatically outputted in JPEG format with 180 dpi resolution. From each image, a squared area (360 × 360 pixel) was cropped as an area of interest (AOI), Fig. 1 and Figs. S1–S2. However, any other predefined AOI can be selected. Thereafter, the AOI was analyzed, using the freeware ImageJ, to obtain the RGB intensities that were converted to the corresponding Y_{xy} and ΔE_{LUV} parameters, based on their excellent responses compared to the original RGB intensities (Mohamed and Shalaby 2019; Mohamed et al. 2018). The color absorbance of x or y parameters and the color difference, ΔE_{LUV}, were calculated from Eqs. (9) and (10), respectively.

$$A_{xy} = \left|\log\left(I_o/I\right)\right| \tag{9}$$

$$\Delta E_{\mathrm{LUV}} = \left[(\Delta L)^2 + (\Delta U)^2 + (\Delta V)^2\right]^{\frac{1}{2}} \tag{10}$$

where I_o and I are the x or y value of the blank and sample, respectively, whereas Δ means the difference in the parameter value between the sample and blank, respectively. For validation, the spectrophotometric cell was placed in the spectrophotometer and spectral curves were recorded, Fig. 2a–c. The [L]/[M] ratio was plotted against the color absorbance of the x or y parameters, Fig. 2d–f, or against the color difference (ΔE) calculated from the LUV color space parameters, Fig. 2g–i.

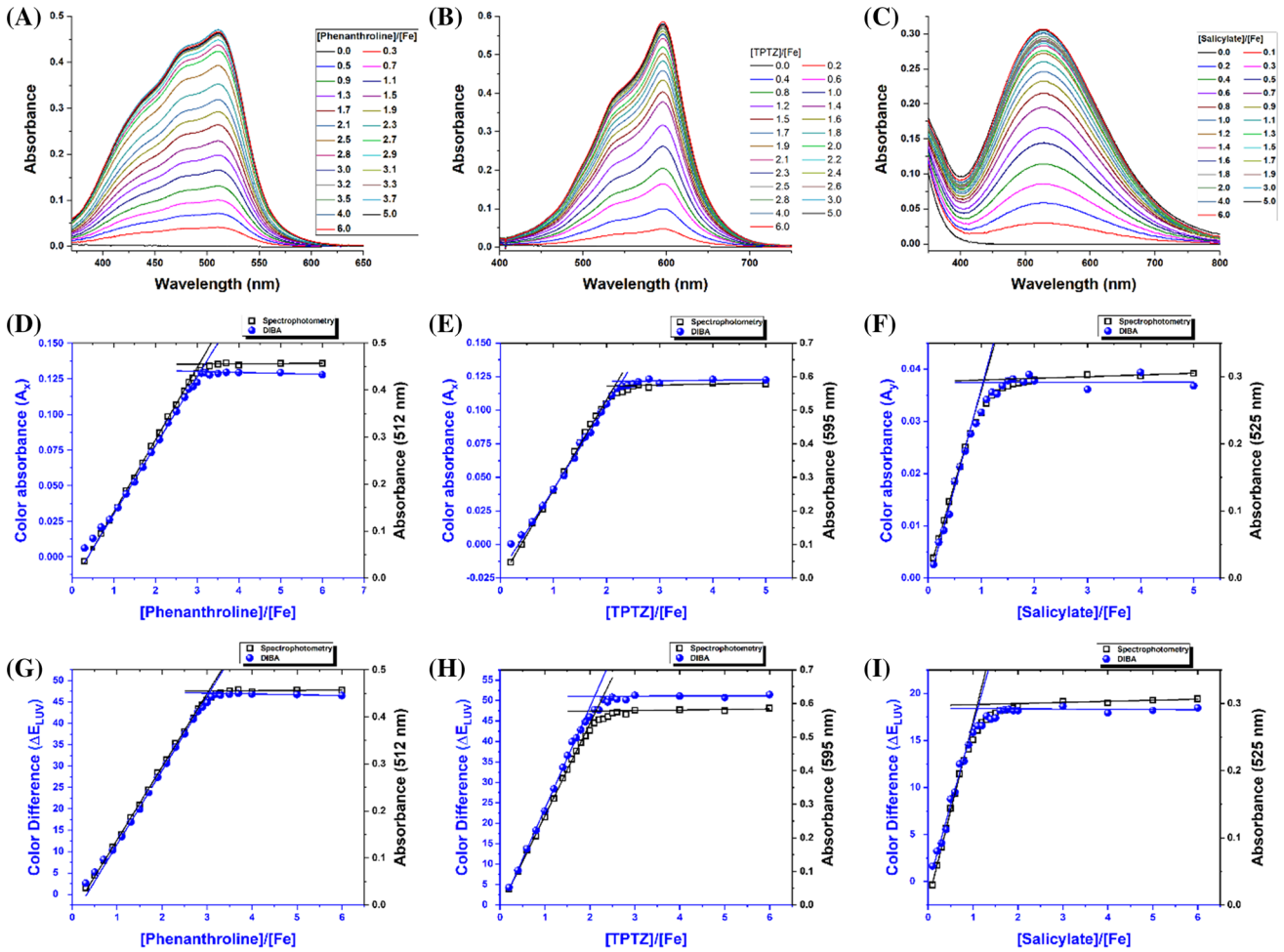

Fig. 2 Spectra obtained at different L:M ratio for the studied Fe complexes with Phenanthroline, TPTZ, and Salicylate (**a**)–(**c**), Molar ratio graphs plotted using spectrophotometric absorbance at the appropriate wavelength and color absorbance of *x* or *y* parameter (**d**)–(**f**), and color difference ΔELUV (**g**)–(**i**). Other conditions were those of Fig. 1

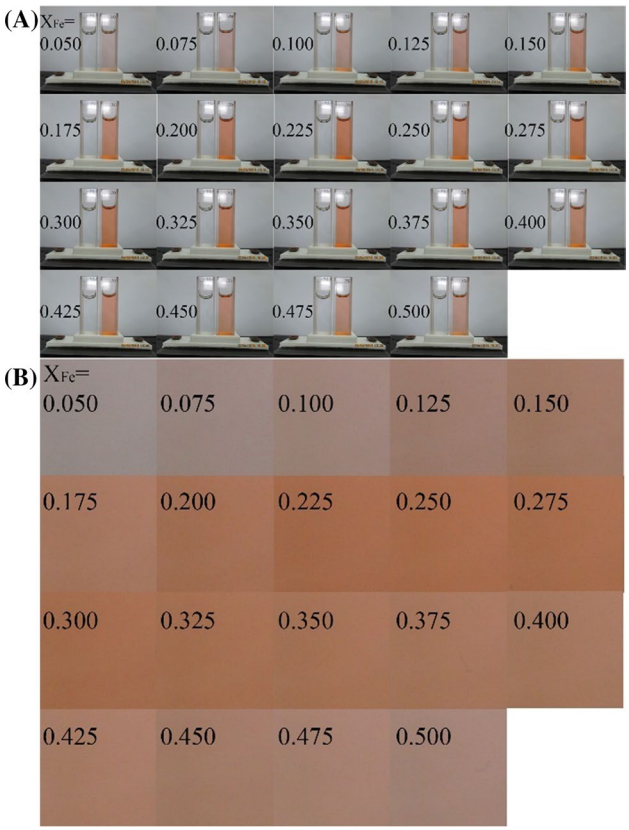

Fig. 3 Digital images of Fe(II)-phenanthroline complex at different Fe(II) mole fraction (**a**) and the cropped Area of interest (**b**). Other conditions were those of Fig. 1

For comparison and validation, the [*L*]/[*M*] ratio was simultaneously plotted against the spectrophotometric absorbance at the appropriate wavelength for each complex, Fig. 2d–i. The DIBA results showed 1:3, 1:2 and 1:1 (*M*:*L*) ratios for the Fe(II)-Phen, Fe(II)-TPTZ and Fe(III)-SAL systems, respectively, in excellent agreement with the spectrophotometric data.

Similarly, in the Job's method of continuous variation, solutions having various mole fractions were prepared for the Fe(II)-Phen, Fe(II)-TPTZ, and Fe(III)-SAL complexes and similarly treated as those of the molar ratio method. Images of these solutions were given in Fig. 3 and Figs. S3–S4, for the Fe(II)-Phen, Fe(II)-TPTZ, and Fe(III)-SAL complexes, respectively. The Job's plots, Fig. 4a–f, of the studies systems exhibited maxima at 0.25, 0.33 and 0.5, for the Fe(II)-Phen, Fe(II)-TPTZ, and Fe(III)-SAL complexes, respectively, showing that iron reacts with phen, TPTZ, and SAL in molar ratios of 1:3, 1:2 and 1:1, respectively. These data reflect the excellent agreement between the spectrophotometric and DIBA measurements.

It's worthy to mention that, in addition to the formed trisphenanthroline-Iron(II) complex ion, other monophenanthroline and diphenanthroline complex ions can be formed. However, compared to the very stable trisphenanthroline complex, the mono- and diphenanthroline complexes are relatively unstable and its existence can be neglected at high phanenthroline-to-Iron(II) ratios. For example, the monophenanthroline-Fe(II) complex is formed only at large

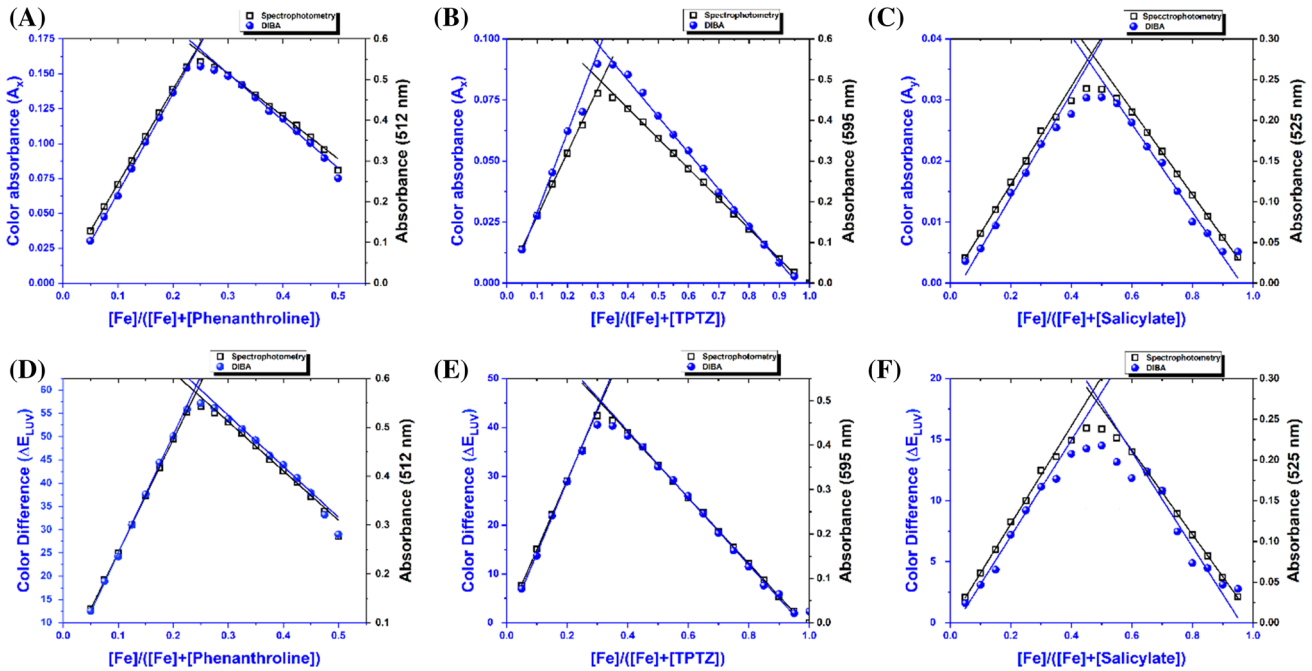

Fig. 4 Continuous variation graphs plotted using the spectrophotometric absorbance and the color absorbance of x or y coordinate of Yxy color (**a**)–(**c**) and color difference ΔELUV (**d**)–(**f**) for the studied Fe complexes with Phenanthroline, TPTZ, and Salicylate. Conditions and symbols were those of Fig. 1

Table 1 Stability constant values of the studied complexes obtained using DIBA and spectrophotometric methods

Complex	Logβ'[a] (I = 0.1, 25 °C)			Logβ[b] (I = 0.1, 25 °C)			Literature value Log β (I = 0.1, 25 °C)
	DIBA (A_{Yxy})	DIBA (ΔE_{LUV})	Spectrophotometry	DIBA (A_{Yxy})	DIBA (ΔE_{LUV})	Spectrophotometry	
Fe(II)-phenanthroline	17.1	17.1	17.2	21.18	21.18	21.28	21.3 (McKenzie 1955) 21.2 (McBRYDE 1978)
Fe(II)- Tris(2-pyridyl)-s-triazine	12.30	12.03	12.19	12.39	12.12	12.28	12.3 (Martell and Smith 1989)
Fe(III)-Salicylate	5.42	5.52	5.43	16.31	16.41	16.32	16.3 (Martell and Smith 1977)

[a]Conditional stability constant

[b]Overall stability constant

excess of ferrous (Kolthoff et al. 1950), so that, it can be formed only at iron mole fraction larger than 0.5 and [phenanthroline]/[Fe] molar ratio less than 1.0.

Further, the conditional and overall stability constants of the three studied complexes were determined from the molar ratio plots using Eqs. (8) and (2), respectively. The side reaction functions of each ligand protonation were calculated from Eq (3) using the previously reported pK_a values for 1,10-phenanthroline (4.84) (CRC handbook of chemistry and physics 2017), TPTZ (3.53 and 2.73) (Martell and Smith 1989), and Salicylic acid (13.6 and 2.98) (CRC handbook of chemistry and physics 2017). The resulting conditional and overall stability constants of the Fe(II)-Phen, Fe(II)-TPTZ, and Fe(III)-SAL complexes, based on spectrophotometric and DIBA measurements are given in Table 1. The data reflects the excellent agreement not only between the DIBA results and the spectrophotometric measurements but also with the previously reported literature values (Chattopadhyaya and Singh 1974; Martell and Smith 1977, 1989; McKenzie 1955). Thus, our simple camera-based platform can be conveniently applied to the determination of complex stoichiometry and stability constants in a manner competing well with the sophisticated spectrophotometers showing its feasibility for practical application in undergraduate students' laboratories.

Conclusions

The stoichiometric ratio and binding constant of metal complexes are important physical and analytical chemistry concepts. Conventional methods for the determination of these parameters often require expensive and/or bulky instruments. Herein, we reported a low-cost and simple approach based on digital imaging. The stoichiometric ratio and binding constants of three iron complexes with 1,10-phenanthroline, 2,4,6-Tris(2-pyridyl)-s-triazine, and salicylate were determined using digital imaging and following the molar ratio and continuous variation methods. The color absorbance of non-uniform Y_{xy} color space and the color difference ΔE_{LUV} derived from the uniform LUV color space were used as convenient analytical signaling tools. The Y_{xy} color absorbance and the ΔE_{LUV} color difference signaling tools can be conveniently applied to investigate a wide range of various colored complexes including not only mononuclear complexes but also polynuclear complexes of various species. Moreover, the current results of composition and conditional and overall stability constants are in excellent agreement with those obtained using sophisticated spectrophotometers and specialized software packages and also in conformity to previously reported literature values. This is very advantageous under resource-limited settings.

Compliance with ethical standards

Conflict of interest On behalf of all authors, the corresponding author states that there is no conflict of interest.

References

Al–Farhan B (2018) Potentiometric and conductometric study of complex formations between Norfloxacin and Some metal ions and Norfloxacin determination in dosage forms. Int J Electrochem Sci. https://doi.org/10.20964/2018.09.43

Ansorge M, Dubsky P, Uselova K (2018) Into the theory of the partial-filling affinity capillary electrophoresis and the determination of apparent stability constants of analyte-ligand complexes. Electrophoresis 39:742–751. https://doi.org/10.1002/elps.201700385

Carmody WR (1964) Demonstrating job's method with colorilneter or spectrophotometer. J Chem Educ 41:615–616. https://doi.org/10.1021/ed041p615

Chattopadhyaya MC, Singh RS (1974) Determination of stability constants of complexes from spectrophotometric data with a digital computer. Anal Chim Acta 70:49–56. https://doi.org/10.1016/s0003-2670(01)82909-3

Chen J, Chen H, Zhang XW, Lei K, Kenny JE (2015) Combination of a copper-ion selective electrode and fluorometric titration for the determination of copper(II) ion conditional stability constants of humic substances. Appl Spectrosc 69:1293–1302. https://doi.org/10.1366/14-07835

Colormine color converter. (2019). http://colormine.org/color-converter. Accessed 27 Jan 2019

CRC handbook of chemistry and physics (2017) 97th edn. CRC Press,Taylor & Francis Group, New York

Cuprys A, Pulicharla R, Lecka J, Brar SK, Drogui P, Surampalli RY (2018) Ciprofloxacin-metal complexes -stability and toxicity tests in the presence of humic substances. Chemosphere 202:549–559. https://doi.org/10.1016/j.chemosphere.2018.03.117

de Morais CDLM, Silva SRB, Vieira DS, Lima KMG (2016) Integrating a smartphone and molecular modeling for determining the binding constant and stoichiometry ratio of the iron(II)–phenanthroline complex: an activity for analytical and physical chemistry laboratories. J Chem Educ 93:1760–1765. https://doi.org/10.1021/acs.jchemed.6b00112

Dömötör O, May NV, Pelivan K, Kiss T, Keppler BK, Kowol CR, Enyedy ÉA (2018) A comparative study of α- N -pyridyl thiosemicarbazones: Spectroscopic properties, solution stability and copper(II) complexation. Inorganica Chimica Acta 472:264–275. https://doi.org/10.1016/j.ica.2017.07.001

Dutta S (2019) Point of care sensing and biosensing using ambient light sensor of smartphone: Critical review TrAC. Trends Anal Chem 110:393–400. https://doi.org/10.1016/j.trac.2018.11.014

Friend MT, Wall NA (2019) Stability constants for Zirconium(IV) complexes with EDTA, CDTA, and DTPA in perchloric acid solutions. Inorg Chim Acta 484:357–367. https://doi.org/10.1016/j.ica.2018.09.034

Gamov GA, Zavalishin MN, Sharnin VA (2019) Comment on the frequently used method of the metal complex-DNA binding constant determination from UV–Vis data. Spectrochim Acta A Mol Biomol Spectrosc 206:160–164. https://doi.org/10.1016/j.saa.2018.08.009

Geiger DK, Pavlak EJ, Kass LT (1991) The determination of axial ligand binding constants for iron porphyrins by cyclic voltammetry. J Chem Educ 68:337–339. https://doi.org/10.1021/ed068p337

Holm R, Østergaard J, Schönbeck C, Jensen H, Shi W, Peters GH, Westh P (2013) Determination of stability constants of tauro- and glyco-conjugated bile salts with the negatively charged sulfobutylether-β-cyclodextrin: comparison of affinity capillary electrophoresis and isothermal titration calorimetry and thermodynamic analysis of the interaction. J Inclusion Phenom Macrocyclic Chem 78:185–194. https://doi.org/10.1007/s10847-013-0287-0

Huangfu C, Zhang Y, Jang M, Feng L (2019) A μPAD for simultaneous monitoring of Cu2 +, Fe2 + and free chlorine in drinking water. Sens Actuators B 293:350–356. https://doi.org/10.1016/j.snb.2019.02.092

Inczédy J (1976) Analytical applications of complex equilibria. ELLIS HORWOOD SERIES IN ANALYTICAL CHEMISTRY. Wiley, New York

Jakusch T et al (2018) Complexes of pyridoxal thiosemicarbazones formed with vanadium(IV/V) and copper(II): Solution equilibrium and structure. Inorganica Chimica Acta 472:243–253. https://doi.org/10.1016/j.ica.2017.08.018

Janrao DM, Pathan J, Kayande DD, Mulla JJ (2014) An over view of potentiometric determination of stability constants of metal complexes. Sci Revs Chem Commun 4:11–24

Kamyabi MA, Soleymani-Bonoti F, Zakavi S (2016) Voltammetric determination of stability constants of lead complexes with diallyl disulfide, dimethyl disulfide, and diallyl sulfide. Chin Chem Lett 27:71–76. https://doi.org/10.1016/j.cclet.2015.09.001

Kazemi MS, Ataeei E, Nasrabadi M (2016) Determination of the stability constant and thermodynamic parameters between Tl +, Ag + and Pb2 + cations with 2,6-di(furyl-2yl)-4-(4-methoxy phenyl) pyridine as a new synthesis ligand. Russ J Electrochem 52:975–982. https://doi.org/10.1134/s1023193516060057

Kluska K, Adamczyk J, Krężel A (2018) Metal binding properties, stability and reactivity of zinc fingers Coordination. Chem Rev 367:18–64. https://doi.org/10.1016/j.ccr.2018.04.009

Kocyla A, Pomorski A, Krezel A (2017) Molar absorption coefficients and stability constants of Zincon metal complexes for determination of metal ions and bioinorganic applications. J Inorg Biochem 176:53–65. https://doi.org/10.1016/j.jinorgbio.2017.08.006

Kolthoff IM, Leussing DL, Lee TS (1950) Reaction of ferrous and ferric iron with 1,10-Phenanthroline. III. The ferrous monophenanthroline complex and the colorimetric determination of phenanthroline. J Am Chem Soc 72:2173–2177. https://doi.org/10.1021/ja01161a083

Martell A, Smith RM (1977) Critical stability constants: other organic ligands vol 3 critical stability constants, vol 3. Springer, New York. https://doi.org/10.1007/978-1-4757-1568-2

Martell AE, Smith RM (1989) Critical stability constants 2nd supplement. Critical stability constants, vol 6. Springer, New York

McBRYDE WAE (1978) A critical review of equilibrium data for proton- and metal complexes of 1,10 phenanthboline, 2,2' bipybidyl and related compounds. IUPAC CHEMICAL DATA SERIES - No. 17, Critical Evaluation of Equilibrium Constants in Solution: Part A: Stability Constants of Metal Complexes. PERGAMON PRESS, Oxford

McKenzie HA (1955) The stability constant of the Tris-1,10-phenanthroline ferrous ion. Aust J Chem 8:569–570. https://doi.org/10.1071/ch9550569

Mohamed AA, Shalaby AA (2019) Digital imaging devices as sensors for iron determination. Food Chem 274:360–367. https://doi.org/10.1016/j.foodchem.2018.09.014

Mohamed AA, Shalaby AA, Salem Abdelnaby M (2018) The Yxy colour space parameters as novel signalling tools for digital imaging sensors in the analytical laboratory. RSC Adv 8:10673–10679. https://doi.org/10.1039/c8ra00209f

Omoto T, Wall NA (2017) Stability constant determinations for technetium (IV) complexation with selected amino carboxylate ligands in high nitrate solutions. Radiochim Acta 105:621–627. https://doi.org/10.1515/ract-2016-2702

Ravichandran R, Rajendran M, Devapiriam D (2014) Antioxidant study of quercetin and their metal complex and determination of stability constant by spectrophotometry method. Food Chem 146:472–478. https://doi.org/10.1016/j.foodchem.2013.09.080

Shokrollahi A, Zarghampour F, Akbari S, Salehi A (2015) Solution scanometry, a new method for determination of acidity constants of indicators. Anal Methods 7:3551–3558. https://doi.org/10.1039/c5ay00287g

Tewari' BB, Singh RKP, Chander R, Yadava KL (1993) Determination Of The Stability Constants Of ZINC(I1) And Cadmium (11) mixed complexes by an electrophoftetlc method. J Natn Sci Coun 21:73–81

Wacker M, Seubert A (2014) Determination of stability constants of strong metal–ligand complexes using anion or cation exchange chromatography and atomic spectrometry detection. J Anal At Spectrom 29:707–714. https://doi.org/10.1039/c3ja50358e

Yoza N (1977) Determining the stability constant of a metal complex by gel chromatography. J Chem Educ 54:284–287. https://doi.org/10.1021/ed054p284